

ARTICLE

## Aging photosynthetic bacteria monitored by absorption and fluorescence changes

Emese Asztalos, Mariann Kis, Péter Maróti\*

Department of Medical Physics, University of Szeged, Hungary

**ABSTRACT** Production and arrangement of photosynthetic pigments into protein complexes were monitored by steady state and kinetic absorption and fluorescence methods in different phases of growth curve of photosynthetic purple bacterium *Rhodobacter sphaeroides*. The increase of the number of pigments (B800, B850 and B875) followed that of the cells and could be described by the modified Gompertz equation. The newly synthesized chromophores were imbedded immediately into the proteinous scaffold independently on the age of the cell (no free pigments were observed). The assembly, however, showed age-dependent changes manifested by slight (~5 nm) blue-shift of the absorption peak of B875 in LH1, by small increase (~10%) of the variable fluorescence and by increased duration of the electrochromic shift detected at 525 nm. The observed changes of the organization of the bacteriochlorophylls in the photosynthetic units upon aging the cell correspond to the tendency of more efficient capture and utilization of light energy.

**KEY WORDS**

growth curves  
photosynthetic pigments  
light harvesting systems  
absorption spectra  
fluorescence induction

Acta Biol Szeged 54(2):149-154 (2010)

The photosynthetic purple bacteria are among of the most ancient and primitive organisms whose bioenergetics has been thoroughly studied and serves as model of more complex energy converting biological systems (Asztalos and Maróti 2009). The antenna pigment proteins in the intracytoplasmic cell membrane (ICM) absorb solar light and transport the energy to the bacterial reaction center (RC), where the light energy is converted into chemical energy directly utilized by the organism (Fig. 1). These antenna molecules are referred to as light harvesting complex 1 (LH1) and light harvesting complex 2 (LH2; Jungas et al. 1999). The LH1 core antenna, a closely coupled pigment system, surrounds the bacterial RC (Jamieson et al. 2002; Roszak et al. 2003). LH1 is, in many types of bacteria, connected to a peripheral antenna, LH2 (Sundstrom et al. 1999). The elementary building block of both LH1 and LH2 is a coupled pair of helical transmembrane polypeptides, the so-called  $\alpha/\beta$  dimer. Both helices bind a bacteriochlorophyll *a* (BChl *a*) at a conserved histidine position (Olsen et al. 1997, 2008), in the case of LH2 the  $\beta$  polypeptide also binds a second Bchl *a* (Waltz et al. 1998). The  $\alpha/\beta$  dimers are arranged in ring like structures. In the case of the LH1 complex of *Rhodobacter (Rba.) sphaeroides* the BChls form two interconnected open rings of 28 dimers in total, with each dimer proposed to have a gate for quinone exchange formed by the PufX protein (Siebert et al. 2004; Qian et al. 2008). In the case of LH2, there is a circular arrangement of 9 dimers binding two concentric rings of 18

B850 BChls and 9 B800 BChls, structurally and energetically connected by carotenoid molecules. While the major interactions that stabilize LH1 are within the  $\alpha/\beta$  subunits, in LH2 the interactions of neighboring amino acids between  $\alpha/\beta$ -pairs are essential. These rings are named according to their absorption maxima, B875 (LH1), B850 (LH2) and B800 (LH2). The LH1 and LH2 have strong internal dipole coupling, exhibit fast transfer between the elements of the ring (a biphasic equilibration of exciton states with lifetimes of ~100 fs and ~400 fs is generally reported), have a big absorption cross section and high structural stability. These properties of the light harvesting system make good candidate to follow structural and functional changes during the cell cycle of the photosynthetic bacteria.

The facultative photoheterotroph purple bacterium *Rhodobacter (Rba.) sphaeroides* is a member of the  $\alpha$ -3 subclass of the *Proteobacteria* (Imhoff 1995) that provides an excellent experimental system to study membrane biogenesis and assembly (Koblizek et al. 2005). When grown under anaerobic conditions in the light, *Rba. sphaeroides* forms a system of intracytoplasmic membranes that house the photosynthetic apparatus. It was shown that the photosynthetic units were assembled in a sequential manner, where the appearance of the LH1-RC cores was followed by the activation of functional electron transfer, and finally by the accumulation of the LH2 complexes. The ICM formation is repressed in the presence of oxygen. The invagination of the cytoplasmic membrane (CM) and the synthesis and assembly of light-harvesting and RC complexes are under the control of a global two-component oxygen sensing, signal transduction system and

Accepted Oct 25, 2010

\*Corresponding author. E-mail: pmaroti@sol.cc.u-szeged.hu

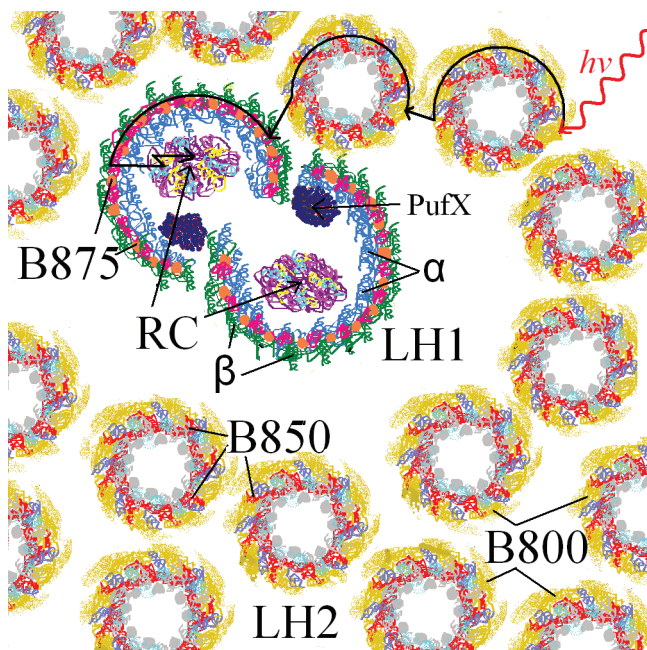


**Figure 1.** Artistic visualization of the photosynthetic light harvesting apparatus of *Rba. sphaeroides* 2.4.1. and migration and capture of the excitation photon  $h\nu$  by the reaction center RC. LH1: light harvesting complex 1, PufX: PufX protein,  $\alpha$  and  $\beta$ : bacteriochlorophyll binding proteins, B875, B850 and B800: bacteriochlorophylls of absorption maxima at 875, 850 and 800 nm bound to  $\alpha/\beta$  dimers, respectively, LH2: light harvesting complex 2.

additional regulatory components (Takemoto and Lascelles 1973; Masuda et al. 2002).

Based on the time evaluation of the concentration of the bacterial cells in the culture, the growth curve of *Rba. sphaeroides* under constant illumination can be divided into lag, exponential, intermediate and stationary phases (De Klerk et al. 1969). We can pose the following simple but not yet properly answered questions: 1) What is the rate of production of the pigments and 2) how do they assemble to functional units (e.g. to light harvesting system) in the different phases of the growth? More frankly, are there any differences between young and old cells in composition and arrangement of the pigments in the light harvesting complexes? We will demonstrate in this paper, that the conventional steady-state absorption spectra of the intact cells at room temperature can hardly answer these questions. The fluorescence characteristics of the pigments, however, will shed some light to and reveal the complexity of this problem.

Methodologically, we can add some novelties to the generally used instrumentation of similar types of physiological studies. Despite the overwhelming use of different chlorophyll fluorometers in functional studies of plants and cyanobacteria (Papageorgiou and Govindjee 2004), the induction of BChl fluorescence of photosynthetic bacteria has

gained interestingly very restricted application (Maróti 2008; Bina et al. 2009; Kocsis et al. 2010). The Kautsky-effect was used to monitor the marine ecosystem (Hohmann-Marriott and Blankenship 2007), the development of the functional photosynthetic units during the growth (aging) of the bacterium cells (De Klerk et al. 1969; Koblizek et al. 2005) and the influence of heavy metal contamination of cultures of photosynthetic bacteria (Asztalos et al. 2010). Here, we display the applicability of variable BChl  $a$  fluorescence transients for elucidating the assemble/dissemble processes of the photosynthetic unit during aging of the bacteria. Beside the conventional absorption techniques, the fluorescence kinetics of intact cells opens new possibilities to reveal up to now hidden aspects of aging.

## Materials and Methods

Cells of purple non-sulfur photosynthetic bacterium *Rhodospira* (*Rba.*) *sphaeroides* strain 2.4.1 were obtained from the German Collection of Microorganisms and Cell Cultures (DSM n. 160) and were cultivated anaerobically in Siström medium (Siström 1962) under stirring in 1 liter screw top flasks at 33°C. The cultures of the bacteria were deoxygenated by bubbling  $N_2$  gas for 15 minutes. Tungsten lamps (40 W) whose spectrum is rich in red components, provided continuous and homogeneous illumination of  $13 \text{ W}\cdot\text{m}^{-2}$  irradiance at the surface of the vessel. The volume of the sample ( $\approx 1.5$  ml) taken regularly was negligible compared to the total volume of the culture and therefore did not modify the growing conditions. The concentration of the cells in the culture was determined by visual counting the number of the sample cells with calibrated Bürker chamber under light microscope.

The steady state spectra of absorption and fluorescence of the cells were measured by Helios  $\gamma$  spectrophotometer (Thermo Electron Corporation) and spectrofluorometer (Perkin Elmer MPF 4) with home-made red-extension of the photodetection by replacing the photomultiplier (Hamamatsu R-446F) by pin photodiode (10DI, UDT Sensors Inc), respectively. The kinetics of light-induced absorption- and fluorescence changes of the whole cells were detected by home-constructed spectrophotometer (Maróti and Wraight 1988) and bacteriochlorophyll fluorometers (Maróti 2008; Maróti and Wraight 2008; Kocsis et al. 2010), respectively.

## Results

### Steady state absorption and fluorescence spectra

Even at room temperature, three bands with center wavelengths of about 800 nm (LH2), 850 nm (LH2) and 875 nm (LH1) can be recognized in the red part of the absorption spectrum of the cells (Fig. 2). After approximation of the baseline originating from intense light scattering by hyperbolic function and subtraction from the measured spectrum,

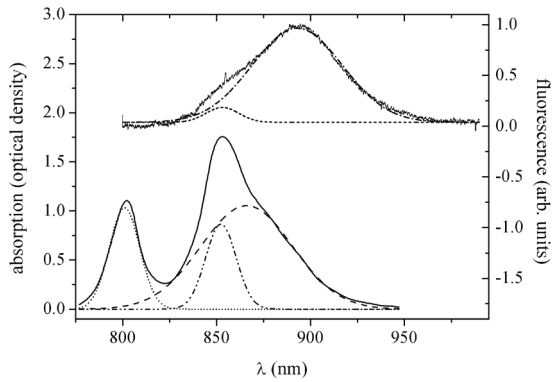


**Figure 2.** Steady state absorption and fluorescence spectra of intact cells of *Rba. sphaeroides*. The absorption spectrum is decomposed into three Gaussian components of peaks at 800 (· · ·), 850 (---) and 875 nm (- · -) and the fluorescence spectrum into two Gaussian components of peaks at 850 nm (· · · · ·) and 895 nm (- · - · -). The blue part of the fluorescence spectrum is cut by a red filter (RG-850).

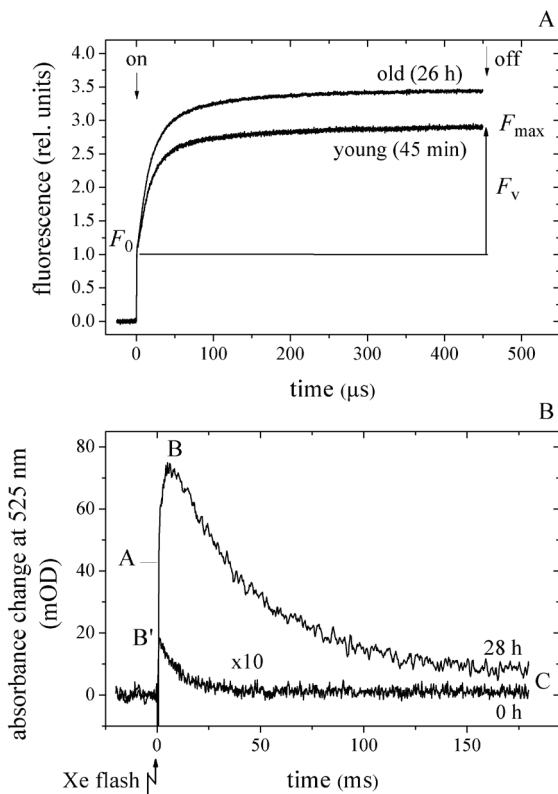


**Figure 3.** Fluorescence induction (A) and kinetics of flash-induced absorption changes (B) of young and old cells of *Rba. sphaeroides* 2.4.1. Panel A: Fluorescence induction kinetics upon stepwise dark-light transition.  $F_0$ ,  $F_v$  and  $F_{max}$  are the dark, the variable and the maximum levels of fluorescence, respectively. The variable fluorescence in young cells is smaller than in old cells. Panel B: Electrochromic signals at 525 nm. (The trace taken at 0 hrs is multiplied by 10.) While the young cells have fast decay kinetics after the small abrupt increase, the old cells have a second and slower increase followed by a slow decay. (For details see Table 1.)

the difference curve was decomposed into the sum of three Gaussian components:

$$(1) \quad y = \sum_{i=1}^3 \frac{A_i}{w_i \sqrt{\pi/2}} \cdot \exp \left[ -\frac{2 \cdot (\lambda - \lambda_{c,i})^2}{w_i^2} \right]$$

where  $A_i$ ,  $w_i$  and  $\lambda_{c,i}$  are the area, the bandwidth and the central wavelength of the  $i$ -th component ( $i=1,2$  and  $3$ ). The Gaussian peeling reveals the dominant role of the core complex (LH1) which cannot be expected from the visual inspection of the spectrum (a shoulder is appearing at the descending part of the spectrum). As the oscillator strength of the component is proportional to the area of the band, this parameter was used to characterize the (absolute and relative) changes of the absorption bands during aging of the bacteria.

The steady-state fluorescence spectrum of the intact cells displays a main band at 895 nm and a satellite band centered at 850 nm that can be also quantified by Gaussian decomposition of the observed spectrum according to Eq. (1).

### Flash induced absorption and fluorescence kinetics

Relatively large absorption change can be detected at 525 nm upon flash illumination in intact cells (Fig. 3). Similar effects were reported in chromatophores of bacteria (Wraight et al. 1978) and utilized widely in algal photosynthesis (Bailleul et al. 2010). The observed changes were attributed to electrochromic shift of marker molecules (e.g. carotenoids) in the membrane. The rise of the signal is due to the energization of the membrane and the decay is characteristics of discharge of the membrane capacitor. Table 1 includes the major kinetic parameters of the electrochromic signals in young and old cells. Note the deceleration of dissipation of the electric field across the membrane upon aging the cells (10 ms  $\rightarrow$  42 ms).

The fluorescence of the cells was obtained by rectangular shape of laser excitation (at 808 nm) and showed typical transient as it increased from  $F_0$  level to  $F_{max}$  level (Fig. 3). As the variable fluorescence ( $F_v = F_{max} - F_0$ ) indicates the photochemical trapping of the excitons in the pigment bed, its ratio to the maximum fluorescence,  $F_v/F_{max}$  characterizes the capability of the bacterium to utilize the excitation (Bina

**Table 1.** (Bi)exponential fit of the flash induced electrochromic kinetics of young and old cells (Fig.3, panel B).

age of the cells (hrs)	rise		decay		
	abrupt (OB' or OA)	slow (AB)	(B'C or BC)	(B'C or BC)	
	amplitude (mOD)	amplitude (mOD)	time (ms)	amplitude (mOD)	time (ms)
young (0)	1.8	–	–	1.8	10
old (28)	27	54	2.3	81	42

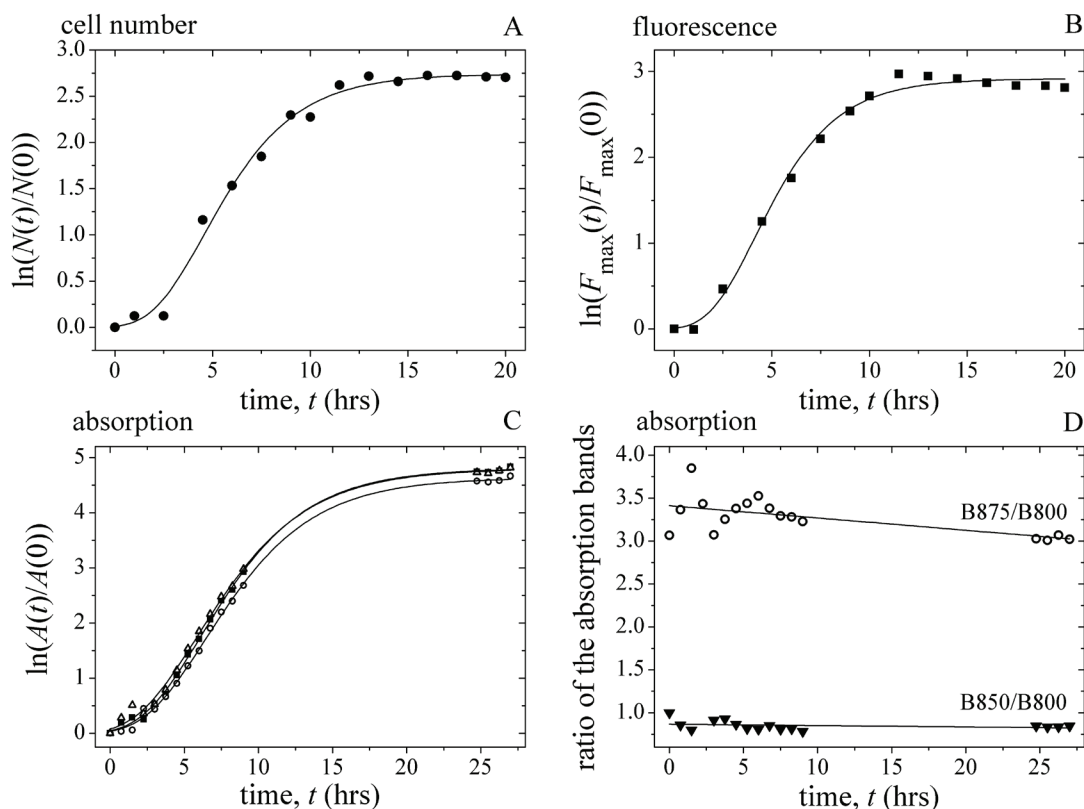


**Figure 4.** Growth curves calculated from cell number (Panel A, ●), from maximum fluorescence level ( $F_{\max}$ ) of the induction (Panel B, ■) and from areas of the Gaussian components (B800 (□), B850 (●) and B875 (▲)) of the absorption spectrum (Panel C) and fitted with the modified Gompertz equation (Eq. (2)). The best fit values are shown in Table 2. Panel D: The ratios of the absorption bands, B875/B800 (○) and B850/B800 (▼) are indicative of the changes of the LH1:LH2 distribution and of the share of the two BChl rings (B850 and B800) within the LH2 complex, respectively.

**Table 2.** Parameters of the growth curves (Fig. 4, panels A-C) fitted by the Gompertz equation (Eq. (2)) using  $N_0$ ,  $N$  and  $N_{\max}$  as initial, actual and asymptotic values of the investigated physical quantity (cell number, fluorescence, absorption or electrochromism), respectively,  $\mu_{\max}$  as maximum rate of doubling and  $\Delta t_0$  as lag time. The cultures used in rows 1 and 2 were different from that used in rows 3 and 4.

physical quantities	initial value	asymptotic value	fitting parameters	
			maximum rate of doubling $\mu_{\max}$ (h <sup>-1</sup> )	$\Delta t_0$ (h)
cell number	$5.5 \cdot 10^8$ cells/ml	$8.2 \cdot 10^9$ cells/ml	0.4	1.9
fluorescence, $F_{\max}$ (rel. units)	1.5	24	0.5	1.8
absorption (area, relative units)	0.18	23	0.44	2.2
B800	0.18	19	0.42	2.4
B850	0.55	68	0.43	1.8
B875				
electrochromism	1.8 mOD	81 mOD	0.7	2.9

et al. 2009; Kocsis et al. 2010). The larger is this ratio (the closer it is to 1), the more effective is the capture of excitation for photochemical purposes.

### Growth curves

The growth curves were obtained by plotting the natural logarithm of the relative increase of the population,  $\ln(N(t)/N_0)$ , against the time,  $t$  elapsed from the inoculation of the cells in the culture medium (Fig. 4). The maximum of growth rate ( $\mu_{\max}$ ), the lag phase duration ( $\Delta t_0$ ) and the asymptotic population size ( $N_{\max}$ ) were determined by fitting the modified Gompertz equation to the growth curves (Zwietering et al. 1990):

$$(2) \quad \ln \frac{N(t)}{N_0} = N_{\max} \cdot \exp \left\{ - \exp \left[ \frac{e \cdot \mu_{\max}}{N_{\max}} (\Delta t_0 - t) + 1 \right] \right\}$$

where  $N(t)$  is the cell concentration at the time  $t$ ,  $N_0$  is the initial cell concentration and  $e$  (the Euler's number) is the base of the natural logarithm. Similar fitting procedures were carried out for the oscillatory strengths of the dipoles (the

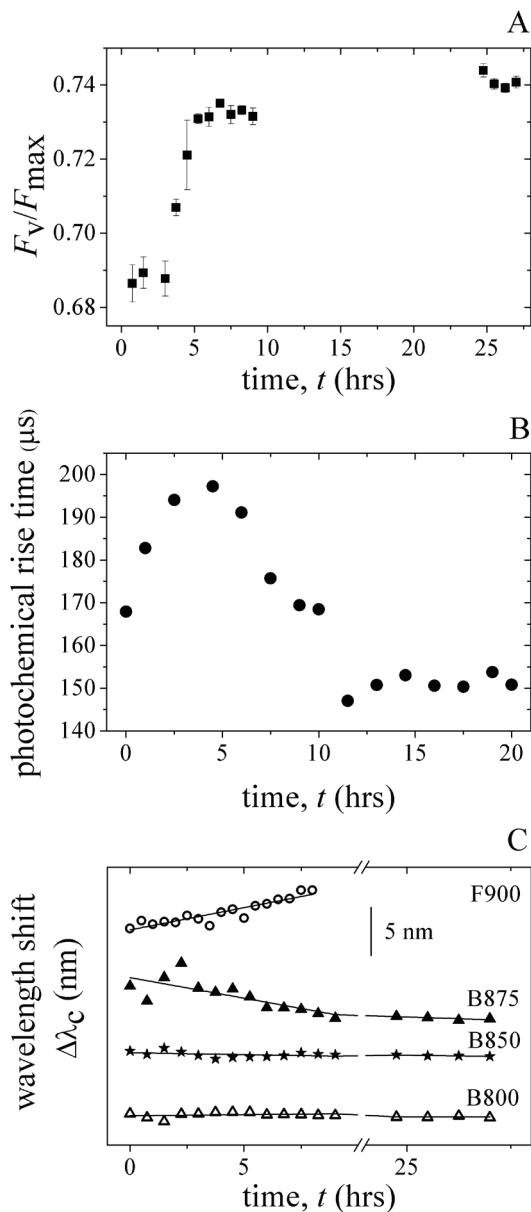


**Figure 5.** Fluorescence induction (A and B) and spectral changes (C) during cultivation of *Rba. sphaeroides* 2.4.1. Panel A: The  $F_V/F_{max}$  ratio shows abrupt rise upon cell division (■) and remains constant even in old cells. Panel B: The photochemical rise time (●) increases in younger cells, then levels off and decreases finally to the initial level in older cells. Panel C: Wavelength shifts of the peaks of characteristic bands during the growth of the bacterial culture. The main fluorescence band F900 shows red shift, the absorption band B875 of LH1 has blue shift and the B800 and B850 bands of LH2 have no changes during the exponential phase of the growth.

band area) of the antenna pigments B800, B850 and B875, for the maximum fluorescence levels after induction  $F_{max}$  and for the magnitude of the electrochromic changes. The fitting parameters are included in Table 2.

## Discussion

The absorption and fluorescence properties of intact bacteria were measured in different phases of the growth to reveal what pigments and at what rate they are produced in the biochemical factories of the organism and how they are assembled into functional units essential to harvest the light and to energize the membrane.

After inoculation of the cells in the culture, the bacteria accommodate to the new conditions (large supply of light and nutrients). All of the investigated parameters show a lag phase of duration about 2 hours. After this transient, the cells divide with high rate (exponential phase, the doubling time is 3 hrs) and the population consists of young (mother and daughter) cells. Upon graduate exhaustion of the food supply, however, the rate of division progressively decreases (intermediate phase) and finally gets zero, *i.e.* no (net) cell division takes place (late stationary phase). These cells can be aged and we call them as old cells. The primary purpose of this study is the comparison of the young and old cells based on spectroscopic characteristics to get easily accessible marks for aging the cells.

Principally, the activity of pigment production and incorporation into protein complexes were in full accordance with the rate of cell division (Fig. 4). We observed slight but definite deviations from this general tendency in some cases only (Fig. 5). 1) The dominance of the core light harvesting complex LH1 compared to the peripheral complex LH2 was stronger in old cells, than in young cells. 2) The fluorescence maximum of the old cells showed red shift of about 5 nm and similar size but blue spectral shift was observed for the B875 pigment. 3) The variable fluorescence was larger by 10% in old bacteria than in young bacteria and the photochemical rise time showed also slight variation indicating moderate changes of the size or connectivity of the antenna system during aging. 4) The old cells performed more stable membrane potential after flash excitation than the younger cells (Fig. 3). As the kinetics of establishment and breakdown of the membrane potential depends on movement of electric charges (electrons, ions and protons) and the dielectric properties (sealing) of the photosynthetic membrane (Baillieul et al. 2010), one can conclude for more sophisticated (finely tuned) dielectrics in old cells than in young cells.

These observations indicate that roughly the same pigments are produced and incorporated into the same protein complexes throughout the growth and no large deviations from this tendency were experienced. That would shed some light of critics on recent conclusions of sequential assembly of photosynthetic units in *Rhodobacter sphaeroides* (Koblizek et al. 2005). If the assembly was sequential *i.e.* the appearance of LH1 was followed by the creation of LH2, then one would expect large changes in the photochemical rate and/or variable fluorescence. As we did not observe the predicted changes in neither phases of the growth curve, the model of parallel pro-

duction and assemble of complexes would be more adequate to our observations. We expect more straightforward proof of the parallel model by performing similar experiments not on asynchronous (as in this study) but on synchronous culture of bacteria under which conditions all cells are brought to the same physiological state.

## Acknowledgements

We are indebted to Dr Tamás Herczeg for the valuable discussions and to Ms Diana Nyúli for preparation of Figure 1. The support of NKTH-OTKA (K-67850), COST Action on “*Molecular machineries for ion translocation across biomembranes*” (CM0902) and MTA-CNR Bilateral agreement on “*Bacterial photosynthesis: artificial photosystems and bioremediation*” is acknowledged.

## References

- Asztalos E, Maróti P (2009) Export or recombination of charges in reaction centers in intact cells of photosynthetic bacteria. *Biochim Biophys Acta* 1787:1444–1450.
- Asztalos E, Italiano F, Milano F, Maróti P, Trotta M (2010) Early detection of mercury contamination by fluorescence induction of photosynthetic bacteria. *Photochem Photobiol Sci* 9:1218–1223.
- Bailleul B, Cardol P, Breyton C, Finazzi G (2010) Electrochromism: a useful probe to study algal photosynthesis. *Photosynth Res* 106:179–189.
- Bina D, Litvin R, Vácha F (2009) Kinetics of in vivo bacteriochlorophyll fluorescence yield and the state of photosynthetic apparatus of purple bacteria. *Photosynth Res* 99:115–125.
- De Klerk H, Govindjee, Kamen MD, Lavorel J (1969) Age and Fluorescence Characteristics in some Species of *Athiorhodaceae*. *Proc Nat Acad Sci* 62:972–978.
- Imhoff JF (1995) Taxonomy and Physiology of Phototrophic Purple Bacteria and Green Sulfur Bacteria, In: *Anoxygenic Photosynthetic Bacteria* (Eds. Blankenship RE, Madigan MT and Bauer CE), Kluwer Academic Publishers, Dordrecht, The Netherlands, pp.1–15.
- Jamieson SJ, Wang P, Qian P, Kirkland KY, Conroy MJ, Hunter CN, Bullough PA (2002) Projection structure of the photosynthetic reaction centre antenna complex of *Rhodospirillum rubrum* at 8.5 Å resolution. *EMBO Journal*, 21(15):3927–3935.
- Jungas C, Ranck J, Rigaud J, Jolliot P, Verméglio A. (1999) Supramolecular organization of the photosynthetic apparatus of *Rhodobacter sphaeroides*. *EMBO Journal* 18(3):534–542.
- Hohmann-Marriott MF, Blankenship RE (2007) Variable fluorescence in green sulfur bacteria. *Biochim Biophys Acta* 1767:106–113.
- Koblizek M, Shih JD, Breitbart SI, Ratcliffe EC, Kolber, ZS, Hunter CN, Niederman RA (2005) Sequential assembly of photosynthetic units in *Rhodobacter sphaeroides* as revealed by fast repetition rate analysis of variable bacteriochlorophyll a fluorescence. *Biochim Biophys Acta* 1706: 220–231.
- Kocsis P, Asztalos E, Gingl Z, Maróti P (2010) Kinetic bacteriochlorophyll fluorometer. *Photosynth Res* 105:73–82.
- Maróti P (2008) Kinetics and yields of bacteriochlorophyll fluorescence: redox and conformation changes in reaction center of *Rhodobacter sphaeroides*. *Eur Biophys J* 37:1175–1184.
- Maróti P, Wraight CA (1988) Flash-induced H<sup>+</sup> binding by bacterial photosynthetic reaction centers: comparison of spectrometric and conductometric methods. *Biochim Biophys Acta* 934:314–328.
- Maróti P, Wraight CA (2008) The redox midpoint potential of the primary quinone of reaction centers in chromatophores of *Rhodobacter sphaeroides* is pH independent. *Eur Biophys J* 37:1207–1217.
- Masuda S, Bauer CE (2002) AppA is a blue light photoreceptor that anti-presses photosynthesis gene expression in *Rhodobacter sphaeroides*. *Cell* 110:613–623.
- Olsen JD, Sturgis JN, Westerhuis WH, Fowler GJS, Hunter CN, Robert B. (1997) Site-directed modification of the ligands to the bacteriochlorophylls of the light-harvesting LH1 and LH2 complexes of *Rhodobacter sphaeroides*. *Biochemistry* 36(41):12625–12632.
- Olsen JD, Tucker JD, Timney JA, Qian P, Vassilev C, Hunter CN (2008) The Organization of LH2 Complexes in Membranes from *Rhodobacter sphaeroides*. *J Biol Chem* 283(45):30772–30779.
- Papageorgiou G, Govindjee (eds) (2004) Chlorophyll a fluorescence: a signature of photosynthesis. *Advances in photosynthesis and respiration*. Springer, Dordrecht, The Netherlands.
- Qian P, Bullough PA, Hunter CN (2008) Three-dimensional reconstruction of a membrane-bending complex - The RC-LH1-PufX core dimer of *Rhodobacter sphaeroides*. *Journal of Biological Chemistry* 283(20):14002–14011.
- Rozsak AW, Howard TD, Southall J, Gardiner AT, Law CJ, Isaacs NW, Cogdell RJ (2003) Crystal structure of the RC-LH1 core complex from *Rhodospseudomonas palustris*. *Science* 302(5652):1969–1972.
- Siebert CA, Qian P, Fotiadis D, Engel A, Hunter CN, Bullough PA (2004) Molecular architecture of photosynthetic membranes in *Rhodobacter sphaeroides*: the role of PufX. *EMBO Journal* 23(4):690–700.
- Siström WR (1962) The Kinetics of the Synthesis of Photopigments in *Rhodospseudomonas sphaeroides*. *J Gen Microbiol* 28:607–616.
- Sundstrom V, Pullerits T, van Grondelle R (1999) Photosynthetic light harvesting: Reconciling dynamics and structure of purple bacterial LH2 reveals function of photosynthetic unit. *J Phys Chem B* 103(13):2327–2346.
- Takemoto J, Lascelles J (1973) Coupling between bacteriochlorophyll and membrane protein synthesis in *Rhodospseudomonas sphaeroides*, *Proc Natl Acad Sci USA* 70: 799–803.
- Walz T, Jamieson SJ, Bowers CM, Bullough PA, Hunter CN (1998) Projection structures of three photosynthetic complexes from *Rhodobacter sphaeroides*: LH2 at 6 Å, LH1 and RC-LH1 at 25 Å. *J Mol Biol* 282(4):833–845.
- Wraight CA, Cogdell RJ, Chance B (1978) Ion Transport and Electrochemical Gradients in Photosynthetic Bacteria. In: *The Photosynthetic Bacteria* (Eds. Clayton RK, Siström WR) Plenum Publishing Corporation 471–511.
- Zwietering MH, Jongenburger I, Rombouts FM, van't Riet K (1990) Modeling of the Bacterial Growth Curve. *Appl Environ Microbiol* 56:1875–1881.